AIChE

Mass Transfer and Separation Criteria for High-Speed Countercurrent Chromatography

Chun-Xia Zhao and Chao-Hong He
State Key Laboratory of Chemical Engineering, Dept. of Chemical and Biological Engineering, Zhejiang University, Hangzhou 310027, China

DOI 10.1002/aic.12282
Published online May 24, 2010 in Wiley Online Library (wileyonlinelibrary.com).

High-speed countercurrent chromatography (HSCCC) is a versatile technique for preparative separations of a wide variety of solutes. For optimization of operating conditions, prediction of separations, and scale-up study, a model is needed to describe the effluent concentration profile, which determines the separation efficiency (mass transfer, mixing, and partitioning) and the resolution between peaks. A transfer-dispersive model is proposed to describe the effluent profile based on the assumption that the retention of a peak is caused by partitioning over two phases, and peak broadening is caused by axial dispersion and mass transfer limitation. In this work, mass transfer was investigated by comparing model simulations to experimental data. One generalized correlation of overall mass transfer coefficients was derived. Based on the correlations of axial dispersion coefficients in our previous work and mass transfer coefficients in this study, the model predicts the elution concentration profile well. Furthermore, separation criteria were proposed to predict the separation of two adjacent solutes, and they were verified using literature data. © 2010 American Institute of Chemical Engineers *AIChE J,* 57: 359–372, 2011

Keywords: high-speed countercurrent chromatography (HSCCC), axial dispersion, mass transfer, partition coefficient, separation criterion

Introduction

High-speed countercurrent chromatography (HSCCC) is a support-free liquid–liquid chromatography, which combines the features of liquid–liquid extraction and partition chromatography. This method provides many advantages over the conventional column chromatography, such as eliminating irreversible adsorption loss of samples, yielding higher recovery and efficiency. As a result, HSCCC has been widely used in chemical and pharmaceutical industries for difficult separation and purification of various natural and synthetic products.[1] Unfortunately, in contrast with the large number of studies on practical applications of HSCCC, there are few studies on the characteristics of the mass transfer kinetics, and much less work has been reported on the modeling of HSCCC processes. However, the development, optimization, and scale-up of a chromatography process largely rely on the quality and precision of the mathematical modeling. Thus, it is becoming increasingly important to model the process. And for being able to optimize the HSCCC separation in a quantitatively way, separation criteria are urgently required that rigorously deal with the complexity of this mass transfer process, and yet can be implemented in such a manner that is simple to use in practice by common users.

With regard to the modeling of chromatography processes, there are two approaches. One is the plate theory, which starts from the assumption of a linear distribution isotherm and phase equilibrium. Kostanian[2] and Kostanian et al.[3] presented a cell model for countercurrent chromatography assuming equilibrium conditions. Sutherland et al.[4] offered a method for modeling CCC on the basis of an eluting countercurrent distribution model. These two models do not deal

Correspondence concerning this article should be addressed to C.-H. He at chhezju@zju.edu.cn.

with the mechanisms of mass transport in the CCC column. Another is the rate theory, which provides the information about the influence of kinetic phenomena such as rate of mass transfer and axial dispersion on the elution profile. van-Buel et al.[5] developed a model for the centrifugal partition chromatography (CPC) to describe the effluent concentration profile. Marchal et al.[6] studied the mass transfer and flow regimes in the CPC using a transparent column and a stroboscopic video system. All these CPC instruments, which depend on hydrostatic equilibrium, are described as not being efficient, and in which the mass transfer limitation is the major reason for peak broadening. However, HSCCC is based on a hydrodynamic equilibrium mechanism, which is totally different from that of CPC instruments. There has been little research on mass transfer in HSCCC, which indicates the need for a model. Furthermore, to the best of our knowledge, no separation criteria have been suggested for determining the chromatographic separations in HSCCC.

Therefore, mass transfer kinetics is investigated in this article using a preparative HSCCC with a 1000-ml column capacity by varying the flow rate, rotation speed, and the two-phase solvent systems, and a generalized correlation of mass transfer is reported. Furthermore, based on the generalized correlations of axial dispersion[7] and mass transfer, separation criteria for HSCCC are proposed and validated using literature data.

Modeling Theory

Numerous mathematical models are available to account for the band profiles obtained in chromatography and in other adsorption-based separation processes.[8–10] When the mass transfer resistances are small and have a minor influence on the profile, the equilibrium-dispersive model is recommended.[10] Otherwise, depending on the nature and the complexity of the problem, the general rate model, the lumped pore diffusion model, or the transport-dispersive (TD) model are used.[11–15] Going through the literature, the authors found that the mathematical description of chromatographic phenomena has already been given by many authors, but the complicated mathematical results had prevented the practical scientists from appreciating the influence of various factors on the performance of chromatographic columns.

In HSCCC, the separation mechanism is based on the difference in partitioning solutes over two immiscible liquid phases, and there is no adsorption–desorption processes. Moreover, the mass transfer resistance has a moderate influence on the profiles of chromatographic bands. Therefore, the TD model is used, which was mentioned in our previous work on a two-phase mode model,[7] but not in detail. In this study, we will elaborate further about this model.

In modeling the effluent concentration profile of a component (chromatogram), the following assumptions are made.

(1) The composition (concentration and type of components) of the injected sample does not influence the partition coefficient of the individual components or the equilibrium composition of the two-phase system, that is, the distribution coefficient is constant. This assumption is usually valid for low component concentrations but may not hold for high concentrations.

(2) The retention of the stationary phase (S_f) is constant at any cross section of the column, and S_f is expressed as:

$$S_f = \frac{V_s}{V_c}, \tag{1}$$

where V_s and V_c are the volumes of stationary phase and the column, respectively.

(3) The temperature is constant.

Based on these assumptions, the resulting set of partial differential equations describing the concentration of a solute in the bulk of the mobile and the stationary phase (C_m and C_s) as a function of the axial position in the column, x, and the time, t, is as follows[6]:

$$\frac{\partial C_m}{\partial t} + \varepsilon \frac{\partial C_s}{\partial t} + u \frac{\partial C_m}{\partial x} = D_{ax} \frac{\partial^2 C_m}{\partial x^2} \tag{2a}$$

$$\frac{\partial C_s}{\partial t} = -k_0 a (C_s - K C_m), \tag{2b}$$

where C_m and C_s are the concentrations of a solute in the mobile and stationary phases, respectively, D_{ax} is the axial dispersion coefficient in the mobile phase, and u is the mean velocity of the mobile phase, which can be calculated as:

$$u = \frac{F}{A_c(1 - S_f)}, \tag{3}$$

where F is the volumetric flow rate of the mobile phase, A_c is the cross-sectional area of the column, and ε is the phase ratio:

$$\varepsilon = \frac{S_f}{1 - S_f} = \frac{V_s}{V_m}, \tag{4}$$

where V_m is the volume of the mobile phase, k_0 is the overall mass transfer coefficient, and a is the specific interfacial area between the mobile and stationary phases.

The boundary and initial conditions are as follows:

$$C_m(0, t) = \begin{cases} C_0 & 0 < t \le t_0 \\ 0 & t > t_0 \end{cases} \tag{5}$$

$$C_m(x, 0) = 0. \tag{6}$$

The solution of these equations, corresponding to the introduction of a concentration pulse $C_0 t_0$ of sufficiently short duration t_0, may be derived from the general solution of Lapidus and Amundson. It reads[16]:

$$C_m(x, t) = \frac{C_0 t_0}{\sqrt{4\pi D_{ax} t^3}} \exp\left[-\frac{(x - ut)^2}{4 D_{ax} t} - \frac{k_0 a t}{1 - S_f} \right] + \int_0^t \frac{x t_0}{\sqrt{4\pi D_{ax} t'^3}} \exp\left[-\frac{(x - ut')^2}{4 D_{ax} t'} \right] F(t') dt', \tag{7}$$

where

$$F(t') = \sqrt{\frac{k_0^2 a^2 K t'}{S_f(1 - S_f)(t - t')}} \exp\left[-\frac{k_0 a K (t - t')}{S_f} - \frac{k_0 a t'}{1 - S_f} \right] \times I_1 \left[2 \sqrt{\frac{k_0^2 a^2 K t' (t - t')}{2 S_f}} \right]. \tag{8}$$

HSCCC instruments are considered as efficient, and more than 1000 theoretical plates are usually encountered. According to van Deemter, Eqs. 7 and 8 can be simplified if the column contains a large number of mixing and transfer units. Therefore, based on the boundary and initial conditions, Eqs. 7 and 8 reduce to a Gaussian function[16]:

$$C_m(L,t) = \frac{C_0 t_0}{\sqrt{4\pi\left(\frac{L(1+\varepsilon\cdot K)^2}{u^3}\cdot D_{ax} + \frac{\varepsilon\cdot K^2\cdot S_f\cdot L}{u}\cdot\frac{1}{k_0 a}\right)}} \exp\left[-\frac{\left(L-\frac{u\cdot t}{1+\varepsilon K}\right)^2}{4\left(\frac{L}{u}\cdot D_{ax} + \frac{\varepsilon\cdot K^2\cdot S_f\cdot L\cdot u}{(1+\varepsilon K)^2}\cdot\frac{1}{k_0 a}\right)}\right]. \quad (9)$$

Equation 9 contains four parameters: S_f, K, D_{ax}, and k_0a (volumetric mass transfer coefficient, considered as one parameter). The retention of the stationary phase S_f can be calculated using the model proposed by the authors,[17] and the partition coefficient K, as the thermodynamic property, could be obtained from shake-flask experiments[5] or calculated by phase equilibrium equations. Axial dispersion coefficients D_{ax} can be calculated according to the model proposed in our previous work,[7] and then the volumetric mass transfer coefficient k_0a can be fitted to the experimental concentration profile with the solutes ($K \neq 0$) according to Eq. 9 with only one unknown parameter k_0a.

Experimental

Apparatus

The HSCCC instrument used in this article is a Model TBE-1000A high-speed countercurrent chromatograph (Tauto Biotech, Shanghai, China) equipped with a 1000-ml coil column made of polytetrafluorethylene tubing (3.0 mm), with a rotor radius of $R = 13$ cm, and a 100-ml sample loop. The coil is wound from head (centre) to tail (periphery) when the mobile phase is pumped into the column in the head–tail mode. The β_r ($\beta_r = r/R$, where r is the distance from the holder axis to the coil, and R is the distance between the holder axis and the central axis of the centrifuge) of the preparative column varies from 0.59 at the internal layer to 0.75 at the external layer. The rotation speed of this apparatus can be regulated with a speed controller in the range between 0 and 600 rpm. The HSCCC system is equipped with a Model SD-9002 constant-flow pump, a HX-2050 water bath, a Model 8823B UV monitor, and a Model N2010 chromatography workstation.

Materials

Three two-phase solvent systems of *n*-hexane–ethyl acetate–ethanol–water at different volume ratios of 8:2:5:5 (4A), 5:5:5:5 (4B), and 3:5:3:5 (4C) have been used, which have a broad range of hydrophobicity. All experiments were conducted in a reverse-phase mode with the aqueous phase as the mobile phase. The solutes used as model components for the three different solvent systems are shown in Table 1.

All organic solvents used for the preparation of samples and HSCCC separations are of analytical grade, and water used is distilled water.

Table 1. Solutes for Different Solvent Systems

Solvent System	Solutes	Octanol–Water Coefficients (log P_{ow})
4A: *n*-Hexane–ethyl	1,2-Hydroxybenzene	0.88
acetate–ethanol–water	Phenol	1.46
(8:2:5:5, v/v)	2-Methylphenol	1.95
4B: *n*-Hexane–ethyl	1,4-Dihydroxybenzene	0.59
acetate–ethanol–water	1,2-Dihydroxybenzene	0.88
(5:5:5:5, v/v)	Phenol	1.46
4C: *n*-Hexane–ethyl	1,2,3-Trihydroxybenzene	0.97
acetate–ethanol–water	1,4-Dihydroxybenzene	0.59
(3:5:3:5, v/v)	1,2-Dihydroxybenzene	0.88

Preparative separation by HSCCC

Preparation of the Two-Phase Solvent System Two-phase solvent systems were prepared by continuously stirring all the solvents according to the volume ratio. After settling at the operating temperature for 12 h, the solvent system was separated into organic and aqueous phases for HSCCC use.

Preparation of the Sample Solution Preparation of the sample solution requires special considerations in order to not affect the HSCCC separation. To maintain the equilibrated phase composition, the sample solution was prepared by dissolving the sample in a solvent mixture containing equal quantities of lower and upper phases (1:1, v/v) of the solvent system. For controlling the partition coefficient under the linear condition, the concentration of the injected samples is in the range of 1–3 g/l.

HSCCC separation procedure

In each experiment, the coiled column was first entirely filled with the upper (stationary) phase, and then the apparatus was rotated at a certain rotation speed, while the lower (mobile) phase was pumped into the column at a certain flow rate. After the mobile phase front emerged and hydrodynamic equilibrium was established in the column, the volume of the stationary phase from the column was measured. Then, the volume of the mobile phase in the column was calculated by subtracting the dead volume[18] (inlet, outlet leads and other peripheral equipment), and the retention of the stationary phase was calculated using Eq. 1. Then, the sample solution containing the solutes was injected through the injection valve. The effluent was continuously monitored with a UV detector. After the separation, the solvents in the column were pushed out by nitrogen gas,[1] and the volumes of upper and lower phases measured as a check on the final retention volume of the stationary phase in the column.

Partition coefficients by shake-flask experiments

Shake-flask experiments[5] were performed to determine the partition coefficient of a component by weighting a small amount into the equilibrated two-phase system ($\pm$10 ml of each phase in a bottle of 50 ml with a Teflon cap) and stirring vigorously overnight in a water bath (25°C). After removal from the water bath, the phases were separated immediately and analyzed by gas chromatography. The experiments were performed in duplicate.

Table 2. Volumetric Mass Transfer Coefficients at Different Operation Conditions

		Volumetric Mass Transfer Coefficient (1/min)								
		4A System			4B System			4C System		
ω (rpm)	F (ml/min)	sm_1	sm_2	sm_3	sm_4	sm_1	sm_2	sm_5	sm_4	sm_1
300	3	0.220	1.629	3.550	0.359	1.382	2.611			
300	5	0.228	1.996	3.416	0.403	1.754	3.077	1.108	1.312	2.892
300	7	0.226	2.095	3.725	0.382	1.636	3.189	1.249	1.431	3.336
300	9	0.231	1.980	3.793	0.339	1.568	3.391	1.224	2.101	3.866
300	11	0.228	2.199	4.246	0.269	1.640	3.536	0.987	1.212	3.218
350	3	0.269	1.983	4.451	0.605	1.737	3.415			
350	5	0.250	2.232	4.016	0.438	2.028	3.639	1.734	1.994	3.898
350	7	0.262	2.474	4.226	0.464	2.029	4.001	1.637	2.125	4.516
350	9	0.258	2.263	4.787	0.441	2.080	4.112	1.533	2.126	4.954
350	11	0.256	2.547	4.476	0.344	2.096	4.413	1.404	1.738	4.510
400	3	0.300	2.516	6.013	0.515	2.101	4.338			
400	5	0.354	2.728	4.577	0.546	2.224	4.027	2.557	2.988	5.295
400	7	0.309	2.846	4.520	0.521	2.351	4.700	2.744	3.092	5.643
400	9	0.276	2.443	5.214	0.490	2.367	4.724	2.591	3.280	6.190
400	11	0.282	2.803	4.940	0.391	2.438	5.183	2.480	3.328	6.191
450	3	0.400	3.323	4.734	0.638	2.222	5.012			
450	5	0.429	3.274	5.623	0.618	2.536	4.641	3.218	3.377	6.059
450	7	0.349	3.215	5.125	0.605	2.740	5.538	3.268	3.681	6.405
450	9	0.305	3.056	5.322	0.584	2.804	5.618	2.829	3.430	7.656
450	11	0.301	2.996	5.299	0.490	3.057	6.521	2.943	3.965	6.804
500	3	0.554	3.602	6.330	0.745	2.924	6.893			
500	5	0.498	3.809	6.728	0.731	2.969	5.497	3.164	3.726	6.271
500	7	0.414	3.793	6.079	0.695	3.151	5.891	3.601	4.327	7.269
500	9	0.327	3.071	5.750	0.689	3.072	6.715	3.407	4.145	8.119
500	11	0.327	3.252	5.781	0.705	3.731	7.073	3.499	4.287	7.644

sm_1: 1,2-hydroxybenzene, sm_2: phenol, sm_3: 2-methylphenol, sm_4: 1,4-dihydroxybenzene, sm_5: 1,2,3-trihydroxybenzene.

Data processing methods

HSCCC chromatogram data were obtained for each sample solution. The flow rate of the mobile phase ranged from 3 to 11 ml/min, and the rotation speed was from 300 to 500 rpm. The experiments were conducted at room temperature of 25°C. The UV detector was set at 254 nm. Before the injection, the UV detector was calibrated.

The experimental concentration of a solute was calculated from the chromatogram. As it is known that there is a linear relationship between the response signal of UV monitor and the solute elution concentration as follows:

$$C = h \cdot b, \tag{10}$$

where h is the chromatogram height, and b is a constant value. The sample mass (M) can be calculated:

$$M = C_0 \cdot V_{\text{inj}} = \int_0^\infty C \cdot dV = \int_0^\infty h \cdot b \cdot d(F \cdot t) = bF \int_0^\infty h \cdot dt = bFA_{\text{chrom}}, \tag{11}$$

where V_{inj} is the sample volume, and A_{chrom} is the chromatogram area. Then,

$$C = \frac{hV_{\text{inj}}C_0}{FA_{\text{chrom}}} = \frac{Mh}{FA_{\text{chrom}}}, \tag{12}$$

Therefore, the solute concentration with time can be calculated from the chromatogram using Eq. 12. As the axial dispersion coefficient D_{ax} is known from our previous work,[7] the volumetric mass transfer coefficient k_0a is fitted to the experimental effluent concentration profile. Optimal values of k_0a can be found by comparison of the experimental and calculated concentrations from Eq. 9. The iterative algorithm was used for searching the optimum k_0a. The minimized objective function "Sum" is the sum of squared deviations between the experimental and calculated concentrations as follows:

$$\text{Sum} = \sum_{j=1}^{N} \left(C_{\text{exp}} - C_{\text{cal}}\right)^2, \tag{13}$$

where C_{exp} is the experimental concentration, C_{cal} is the calculated concentration, and N is the number of data points.

Results and Discussion

Volumetric mass transfer coefficient

Three sets of experiments were performed using three different solvent systems listed in Table 1 with varying the flow rate from 3 to 11 ml/min and the rotation speed from 300 to 500 rpm. As the elution time (about 12 h) for the flow rate of 3 ml/min was too long for the 4C system, the experiments were only performed for four flow rates of 5, 7, 9, and 11 ml/min. The overall volumetric mass transfer coefficients were determined by fitting to the effluent concentration profiles, as described in the data processing methods. The overall volumetric mass transfer coefficients of 1,2,3-trihydroxybenzene, 1,4-dihydroxybenzene, 1,2-dihydroxybenzene, phenol, and 2-methylphenol in three different solvent systems are shown in Table 2.

Figure 1 shows the volumetric mass transfer coefficients of pyrocatechol as a function of the rotation speed with

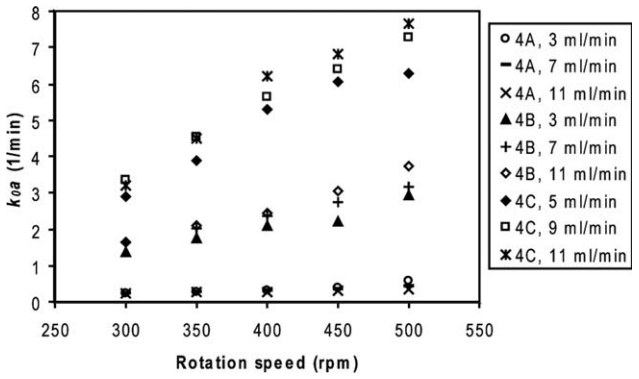

Figure 1. Overall volumetric mass transfer coefficients (K_0a) vs. rotation speed in three solvent systems.

varying the flow rate in the three different solvent systems. It can be noted that the overall mass transfer increases greatly with the rotation speed but nearly keeps constant with the flow rate, which agrees with the tendencies of axial dispersion coefficients with the flow rate and rotation speed in our previous work.[7] Moreover, the solvent system has a great influence on the volumetric mass transfer coefficient. As shown in Figure 1, the overall mass transfer coefficients are the largest for the 4C system and the smallest for the 4A system. Furthermore, it is very interesting to find (Table 2) that the overall mass transfer coefficients of 1,4-dihydroxybenzene and 1,2-dihydroxybenzene, a pair of isomeric compounds, are of significant difference in 4B and 4C systems, which is due to the different partition coefficients because all the conditions including the solvent system and operating conditions (flow rate and rotation speed) are exactly the same for the two isomeric solutes except the different K values. Therefore, it can be known that the overall mass transfer coefficients in HSCCC are dependent on the rotation speed and the partition coefficient.

Mass transfer as a function of Re and Sc

The volumetric mass transfer coefficient k_0a in Eq. 9 is the product of the mass transfer coefficient k_0 and the specific interfacial area a. It is very difficult to measure the specific interfacial area a directly because of the complexity of the HSCCC separation; therefore, k_0a are lumped together. The values of k_0a are expressed in the form of a modified Sherwood number (Sh')[19]:

$$Sh' = \frac{k_0 a d^2}{D} = Sh \cdot a \cdot d, \tag{14}$$

where Sh is the Sherwood number (Sh),

$$Sh = \frac{k_0 d}{D}, \tag{15}$$

where d is the characteristic length scale of mass transfer (herein expressed as the internal diameter of the HSCCC column), and D is the molecular diffusion coefficient of the solute. The product of a and d is combined into the Sherwood number as a dimensionless parameter.

Correlations describing mass transfer coefficients are very important in the design of mass transfer equipment, and HSCCC is no exception. Usually, the mass transfer coefficient in a single phase can be correlated using this dimensionless correlation form as follows:

$$Sh'_{\mathrm{m}} = x_1 Sc^{x_2} Re^{x_3}, \tag{16}$$

where Sh'_{m} is the modified Sherwood number of the mobile phase. Equation 16 relates the modified Sherwood number (Sh') in the mobile phase, a function of the mass transfer coefficient, to the Schmidt (Sc) and the Reynolds (Re) numbers of the mobile phase. These dimensionless parameters are defined in HSCCC as:

$$Sh'_{\mathrm{m}} = \frac{k_{\mathrm{m}} a d^2}{D_{\mathrm{m}}} \tag{17}$$

$$Sc = \frac{\mu_{\mathrm{m}}}{\rho_{\mathrm{m}} D_{\mathrm{m}}} \tag{18}$$

in which μ_{m} is the viscosity of the mobile phase, ρ_{m} is its density, k_{m} is the mass transfer coefficient in the mobile phase, and D_{m} is the molecular diffusion coefficient of the solute in the mobile phase. This relationship permits the calculation of k_{m} knowing the molecular diffusivity D_{m}. Usually, D_{m} can be estimated by the Wilke-Chang equation.[20]

The overall mass transfer coefficient k_0 is related to the individual mass transfer coefficients, which typically cannot be measured directly:

$$\frac{1}{k_o} = \frac{1}{k_{\mathrm{m}}} + \frac{1}{K \cdot k_{\mathrm{s}}}, \tag{19}$$

where k_{s} is the mass transfer coefficient of the solutes in the stationary phase. There are two limiting cases:

(1) When $\frac{1}{k_{\mathrm{m}}} \rangle\rangle \frac{1}{k_{\mathrm{s}}}$, then $k_o \approx k_m$. In this case, the solute prefers the stationary phase, and the mobile phase is the "mass transfer limiting" phase. The overall mass transfer coefficient k_0 is independent of the partition coefficient K.

(2) When $\frac{1}{k_{\mathrm{m}}} \langle\langle \frac{1}{k_{\mathrm{s}}}$, then $k_o \approx K \cdot k_{\mathrm{s}}$. In this case, the solute prefers the mobile phase, and the stationary phase is the "mass transfer limiting" phase. The overall mass transfer coefficient k_0 has a linear relationship with the partition coefficient K.

Aside from these two limiting cases, there is another condition sitting in the middle of them, that is,

(3) When $\frac{1}{k_{\mathrm{m}}} \approx \frac{1}{k_{\mathrm{s}}}$, the solute favors approximately equal to the stationary and mobile phases. Therefore, the overall mass transfer coefficient k_0 is approximately described as:

$$k_0 = \frac{K}{K+1} k_{\mathrm{m}}. \tag{20}$$

The first case is not true because the overall volumetric mass transfer coefficient k_0a has been proved to be dependent on the partition coefficient K in our experiments (as described above in the "volumetric mass transfer coefficient" section), but not a linear relationship. Therefore, the second case does not apply either. As the solute in the spiral column is subjected to the repetitive partition process of

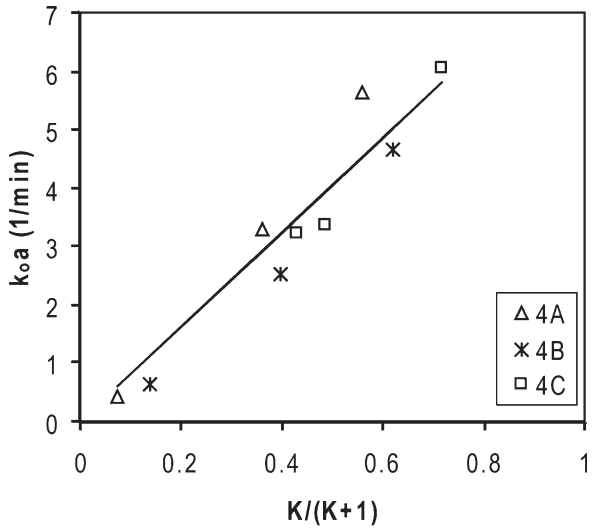

Figure 2. Overall volumetric mass transfer coefficient as a function of K/(K + 1) for 4A, 4B, and 4C systems at the flow rate of 5 ml/min and rotation speed of 450 rpm.

mixing and settling at an enormously high rate of over 13 times per second (at 800 rpm),[1] the concentration of solutes in both the dispersed and continuous phase tends to be the equilibrium state very quickly. Thus, the resistances from both phases are quite close. Consequently, it could be reasonably proposed that these two individual mass transfer coefficients are approximately equal. For validating Eq. 20, the relationship between the overall volumetric mass transfer coefficient k_0a and $K/(K + 1)$ is shown in Figure 2. As it is expected, the result agrees well with Eq. 20, which validates our initial hypothesis.

Then, the modified Schmidt number based on the overall volumetric mass transfer coefficients k_0a is

$$Sh' = \frac{k_0 a d^2}{D} = \frac{k_m a d^2}{D} \cdot \frac{K}{K+1} = x_1 Sc^{x_2} Re^{x_3} \cdot \frac{K}{K+1}. \quad (21)$$

The parameter x_2 in Eq. 21 represents the characteristics of solvent systems (μ_m, ρ_m) and solutes (D_m), so the exponent of 1/3 of Schmidt number in usual conditions can be used,[21] that is, $x_2 = 1/3$. The relationship between the mass transfer coefficient and *Re* number can be approximately estimated with Danckwerts's surface renewal theory[21]:

$$k_m = \sqrt{D_m s}, \quad (22)$$

where s is the surface renewal factor, which is dependent on the flow rate of the liquid,[22] the high rotation speed in HSCCC also contributes to the surface renewal factor. Usually, the surface renewal factor s increases with the velocity of the mobile phase and the rotation speed. Therefore, it can be assumed that

$$s \propto u \cdot \omega. \quad (23)$$

According to the relationship between the retention of the stationary phase S_f and the volumetric flow rate of the mobile phase F and the rotation speed ω,[17] and the linear relationship between $(1 - S_f)$ and $1/d^2$ proposed by Wood et al.,[23]

$$1 - S_f \propto \frac{1}{d^2} \cdot \frac{\sqrt{F}}{\omega}. \quad (24)$$

The velocity of the mobile phase u will be:

$$u = \frac{F}{A_c(1 - S_f)} = \frac{4Fd^2\omega}{\pi d^2 \sqrt{F}} \propto \sqrt{F} \cdot \omega \quad (25)$$

then

$$k_m \propto \sqrt{D_m \sqrt{F} \omega^2} \propto F^{1/4} \cdot \omega. \quad (26)$$

From Eq. 26, it can be noted that in comparison with the rotation speed, the influence of the flow rate on the mass transfer of the mobile phase is quite small. Along with the experiment results that the overall mass transfer coefficient is mainly influenced by the rotation speed (Figure 1), the Reynolds number in Eq. 21 is regarded as the rotational Reynolds number Re_ω ($\mathrm{Re}_\omega (= \frac{\rho_m d(R\omega)}{\mu_m})$), which was defined in our previous work,[7] and the exponent of Re x_3 in Eq. 21 is designated as unity according to Eq. 26. Therefore, the correlation between Sh' and Sc, Re_ω becomes:

$$Sh' = m_1 Sc^{1/3} Re_\omega \frac{K}{K+1}. \quad (27)$$

The experimental relationship between Sh' and $Sc^{1/3}Re_\omega \cdot \frac{K}{K+1}$ is shown in Figure 3. It agrees well with Eq. 27, which validates our theoretical analysis described above. And, the parameter m_1 was obtained as following:

$$m_1 = 6.50 \times 10^{-3}. \quad (28)$$

Then, Eq. 27 becomes:

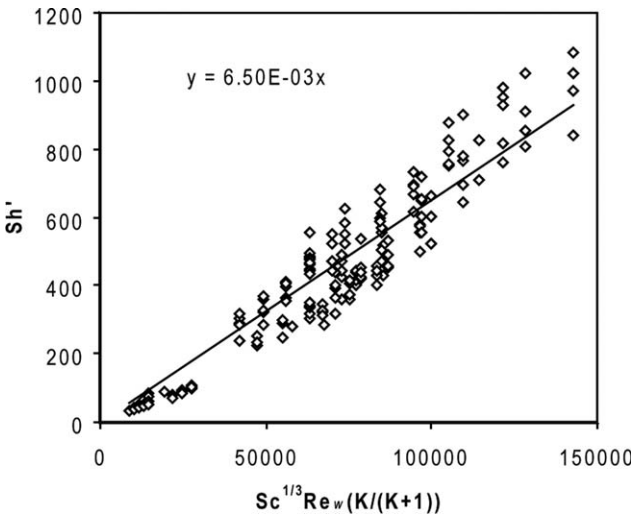

Figure 3. Relationship between Sh′ and $Sc^{1/3}Re_\omega \cdot \frac{K}{K+1}$.

$$Sh' = 6.5 \times 10^{-3} Sc^{1/3} Re_\omega \frac{K}{K+1}, \quad (29)$$

where, $800 < Sc < 1200$, $1 \times 10^4 < Re_\omega < 2.5 \times 10^4$, and $0 < K < 2.5$.

Prediction of elution concentration profiles

According to the axial dispersion coefficient model[7] and the mass transfer coefficients model Eq. 29, the axial dispersion coefficient D_{ax} and the volumetric mass transfer coefficient k_0a can be calculated, and then the elution concentration profile of a solute can be predicted using Eq. 9.

The model (Eq. 9) was used to predict the effluent concentration profile using our preparative HSCCC. It is found that the agreement between the prediction and the experimental data is fairly good using three systems including common or natural bioactive substances separated using the HSCCC instrument in our laboratory. Furthermore, the validity of the proposed model for other HSCCC apparatuses needs to be verified. The axial dispersion model[7] reported in our previous article did not involve the HSCCC apparatus parameter (L/d) because of the limitation of apparatus availability in our laboratory. Based on Taylor's theory, the dimensionless Peclet number has a linear relationship with the aspect ratio (L/d) in a single-phase flow as follows[24]:

$$Pe \propto \left(\frac{L}{d}\right), \quad (30)$$

where the Peclet number is expressed as:

$$Pe = \frac{uL}{D_{ax}}. \quad (31)$$

Then, our correlation for the axial dispersion in HSCCC,[7]

$$Pe = 3.005 \times 10^8 \cdot \frac{Re^{0.374}}{Re_\omega^{1.302}}. \quad (32)$$

In combination with the column aspect ratio (L/d) gives:

$$Pe = \frac{3.005 \times 10^8}{(L/d)} \cdot \frac{Re^{0.374}}{Re_\omega^{1.302}} \cdot \left(\frac{L}{d}\right) = 6.066 \times 10^3 \cdot \frac{Re^{0.374}}{Re_\omega^{1.302}} \cdot \left(\frac{L}{d}\right). \quad (33)$$

Then

$$\frac{ud}{D_{ax}} = 6.066 \times 10^3 \cdot \frac{Re^{0.374}}{Re_\omega^{1.302}}. \quad (34)$$

From Eqs. 34 and 29, the axial dispersion coefficients D_{ax} and the volumetric overall mass transfer coefficients k_0a are only dependent on the column diameter d, not on the column length L. As we know the resolution (Rs) in common chromatography changes directly with the square root of the ratio of the column length (L), which is also demonstrated in HSCCC,[25]

$$\mathrm{Rs}_2 = \mathrm{Rs}_1 \cdot \left(\frac{L_2}{L_1}\right)^{0.5}, \quad (35)$$

where Rs_1 and Rs_2 are resolutions for the columns with length L_1 and L_2, respectively. The peak resolution Rs, that is, the separation of two peaks in terms of their average peak width at baseline ($t_2 > t_1$),

$$\mathrm{Rs} = \frac{t_2 - t_1}{(w_2 + w_1)/2} = \frac{2(t_2 - t_1)}{(w_2 + w_1)}, \quad (36)$$

where t_1 and t_2 are the retention times of substances 1 and 2, respectively, and w_2 and w_1 is the baseline peak widths of substances 1 and 2, respectively. In HSCCC, the retention time t is

$$t = \frac{V_c}{F}[(1 - S_f) + S_f K] = \frac{L\pi d^2}{4F}[(1 - S_f) + S_f K]. \quad (37)$$

From Eq. 9, the peak width w is[7]

$$w = 4\sigma = 4 \times \sqrt{2\left(\frac{L}{u} D_{ax} \cdot \frac{(1+\varepsilon K)^2}{u^2} + \frac{\varepsilon K^2 S_f L}{u} \cdot \frac{1}{k_0 a}\right)}. \quad (38)$$

If D_{ax} and k_0a are independent of L, substituting t and w into Eq. 35 with Eqs. 36 and 37 gives

$$\mathrm{Rs} \propto L^{1/2}. \quad (39)$$

This relationship between Rs and L in Eq. 39 agrees well with the results of Eq. 35 from the literature,[25] which to some extent demonstrates the validity of our model. Therefore, our model was used to test the separation of other types of HSCCC apparatuses. The prediction of elution concentration profiles by using Eqs. 29, 34, and 9 for five systems[26–30] were compared, and the agreement between the experimental and predicted data is good. As typical examples, the detailed comparisons between the experimental data and the calculated results are shown in Figure 4, including the literature data for an analytical HSCCC (V_c = 36 ml),[28] a semipreparative (V_c = 325 ml)[27] HSCCC, and the experimental data for our preparative HSCCC (V_c = 1000 ml).[29] It is proved that the calculated elution profiles agree well with the experimental data. Therefore, the model proposed in this study would be very helpful for choosing appropriate solvent systems and optimizing the HSCCC separation.

Separation criteria

The prediction of an elution profile is very useful to obtain detailed information about the retention time, peak width, and resolution as well, but it takes a long time and needs complicated calculations. Hence, it would be very helpful if some separation criteria were available to predict whether two substances can be separated or not. Generally, baseline resolution is achieved if $Rs \geq 1.5$, based on the definition of Rs, it gives

$$2(t_2 - t_1) \geq 1.5 \times (w_2 + w_1). \quad (40)$$

Substituting Eqs. 37 and 38 into Eq. 40 gives

$$3 \times \sqrt{2\left(A \cdot \left(\frac{1}{\varepsilon K_2} + 1\right)^2 + B \cdot \left(1 + \frac{1}{K_2}\right)\right)} + 3 \times \sqrt{2\left(A \cdot \left(\frac{1}{\varepsilon K_2} + \frac{K_1}{K_2}\right)^2 + \frac{B \cdot K_1}{K_2^2}(K_1 + 1)\right)} + \frac{K_1}{K_2} \leq 1, \quad (41)$$

where A and B are as follows:

$$A = \frac{d}{L} \cdot \frac{Re_\omega^{1.302}}{3.005 \times 10^8 Re^{0.374}} \quad (42)$$

$$B = \frac{(1 - S_f)u}{L} \cdot \frac{d^2 \rho_m^{1/3}}{6.5 \times 10^{-3} (\mu_m)^{1/3} Re_\omega D_m^{2/3}} \quad (43)$$

Designate Y_1

$$Y_1 = 3 \times \sqrt{2\left(A \cdot \left(\frac{1}{\varepsilon K_2} + 1\right)^2 + B \cdot \left(1 + \frac{1}{K_2}\right)\right)} + 3 \times \sqrt{2\left(A \cdot \left(\frac{1}{\varepsilon K_2} + \frac{K_1}{K_2}\right)^2 + \frac{B \cdot K_1}{K_2^2}(K_1 + 1)\right)} + \frac{K_1}{K_2}. \quad (44)$$

When $Y_1 \leq 1$, baseline separation between two peaks can be achieved. Compared with the calculation of elution profiles, it is more convenient by using Eqs. 41–43. However, even for the most simple case of separating two substances, all the parameters, including flow rate, rotation speed, density and viscosity of the solvent system, and retention of the stationary phase, are required to carry out the calculation, and this does not meet our needs "quick and easy to use." To simplify this problem, we attempt to compare the Y_1 values at different operating conditions (flow rate and rotation speed) for different solvent systems. Small flow rate and big rotation speed usually gave better peak resolutions, but when keeping on decreasing the flow rate and increasing the rotation speed to certain values, the peak resolution cannot be improved any more. Figure 5 indicates that the flow rate decreasing from 3 to 1 ml/min does not significantly change Y_1, but the separation time for the substance, for instance, with $K = 1$, increases twofold from 333.3 to 1000 min, and such a long time is not usually acceptable for a separation. The influence of the rotation speed on Y_1 values is negligible from 450 to 600 rpm as seen in Figure 5. Furthermore, the higher rotation speed may build up more pressure in the column. Therefore, two extreme operating conditions: rotation speed of 300 rpm and flow rate of 11 ml/min (300-11), which represents the worst separation condition in our systems and rotation speed of 500 rpm and flow rate of 3 ml/min (500-3), the best separation condition, were compared for 4A, 4B, and 4C systems. As shown in Figure 6, when the partition coefficient of the less retained substance K_1 is less than 0.2, the solvent system has great influence on the separation of substances (here K_1 is less than K_2 from Eq. 36 of $(t_2 - t_1)$). However, all the data fall onto two separate curves when K is bigger than 0.3, and Y_1 values do not vary with the solvent systems. Furthermore, comparing with the separation at 300-11 (300 rpm, 11 ml/min), the influence of

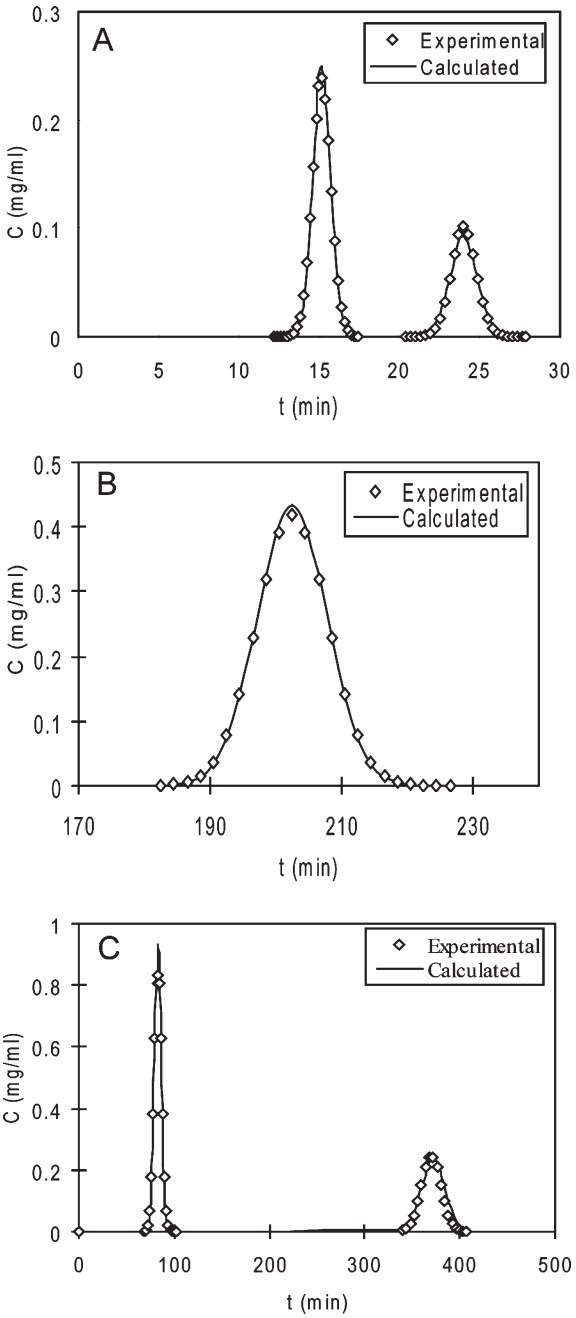

Figure 4. Calculated results of HSCCC elution concentration profile comparing to the experimental result.

(A) Standard honokiol and magnolol by analytical CCC (V_c = 36 ml, d = 1.2 mm)[26]; (B) Separation of phillyrin from the medicinal plant *Forsythia suspense* by semipreparative CCC (V_c = 325 ml, d = 2.6 mm)[25]; (C) Separation of atractylenolide III and atractylon[27] by preparative HSCCC (solvent system: hexane–ethyl acetate–ethanol–water, 4:1:4:1, v/v, flow rate: 5 ml/min, rotation speed: 450 rpm; V_c = 1000 ml, d = 3 mm).

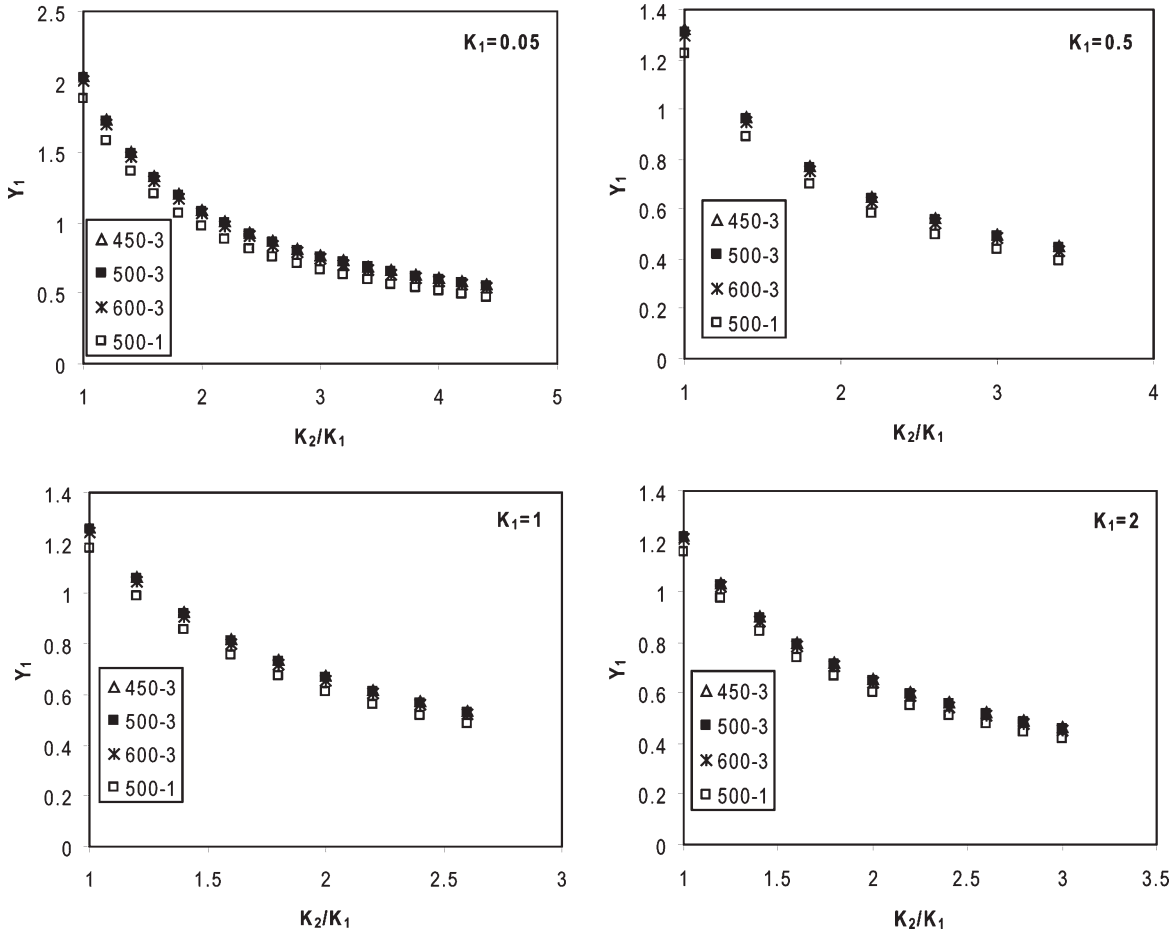

Figure 5. Influence of flow rate and rotation speed on separation criteria Y_1 in 4A system.

450-3: rotation speed of 450 rpm, flow rate of 3 ml/min; 500-3: rotation speed of 500 rpm, flow rate of 3 ml/min; 600-3: rotation speed of 600 rpm, flow rate of 3 ml/min; and 500-1: rotation speed of 500 rpm, flow rate of 1 ml/min.

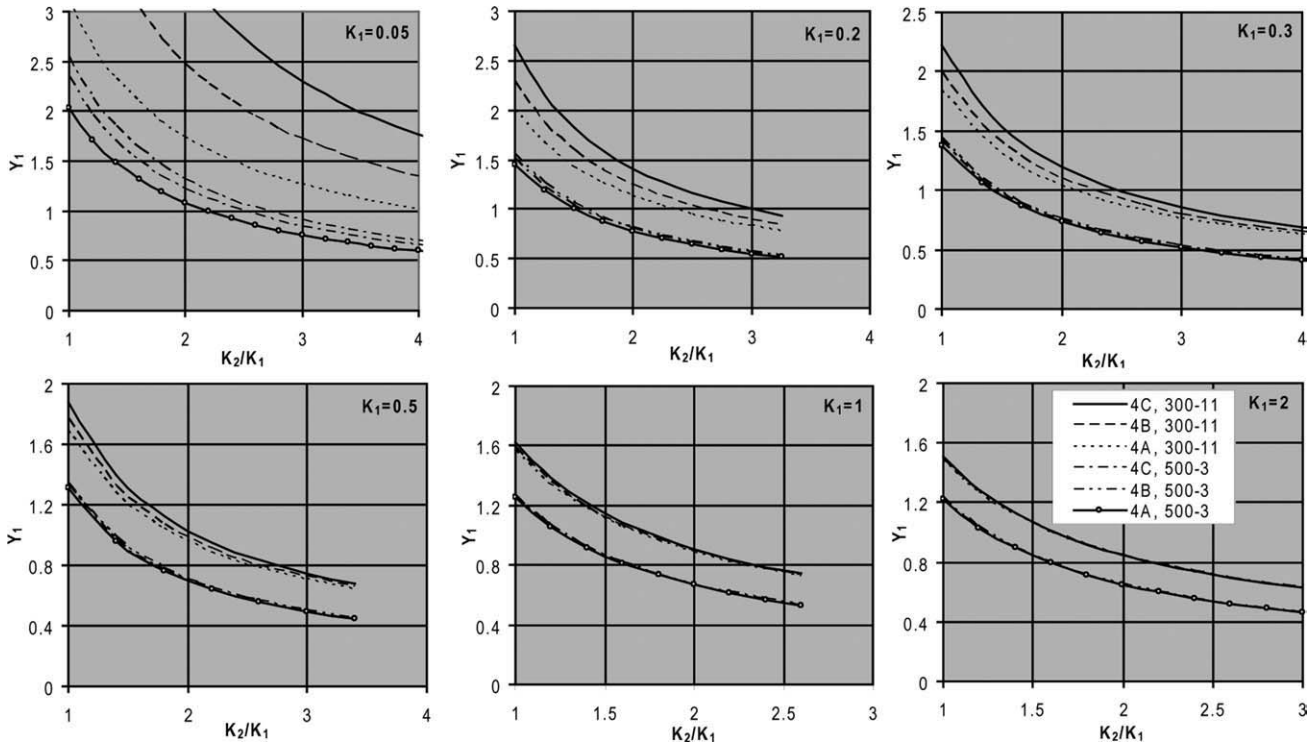

Figure 6. Partition coefficient ratio vs. separation parameter Y_1 for the worst separation conditions (300-11: rotation speed of 300 rpm, flow rate of 11 ml/min) and the best separation conditions (500-3: rotation speed of 500 rpm, flow rate of 3 ml/min) for three different solvent systems 4A, 4B, and 4C.

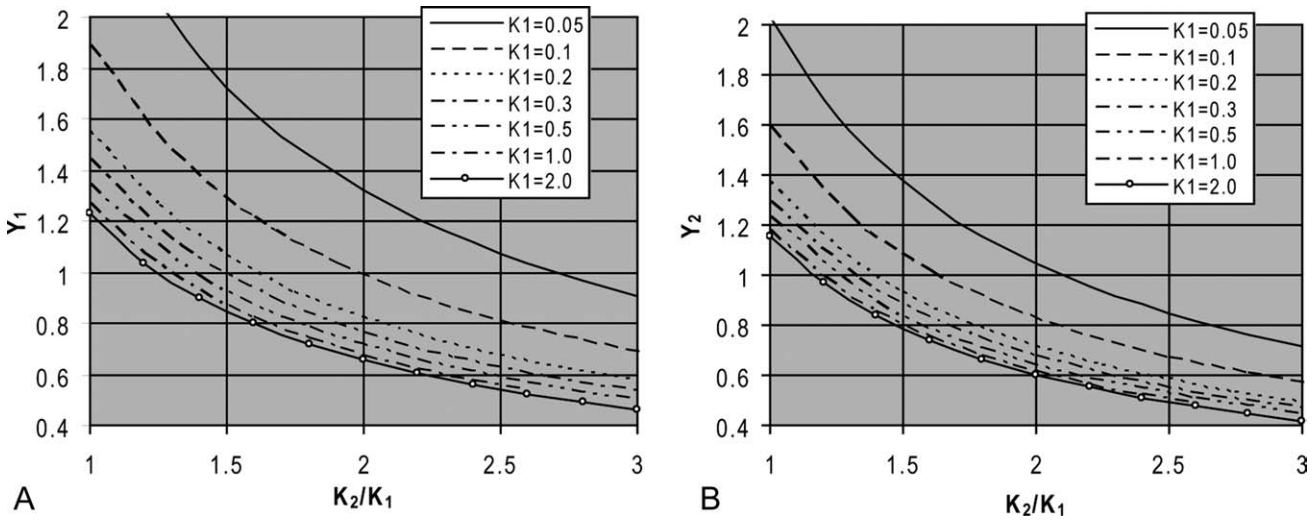

Figure 7. Separation criteria Y_1 and Y_2 of adjacent peaks for the best separation condition from Figure 6 for phase system 4B only.

(A) Baseline separation criterion and (B) acceptable separation criterion.

solvent systems is insignificant for 500-3 (500 rpm, 3 ml/min), and the three curves of 4A, 4B, and 4C systems for 500-3 are quite close to each other over the whole range of partition coefficients. As we are more interested in the best conditions which can provide good separation results than worst conditions, eliminating the worst separation condition and keeping the best conditions lead to a significant simplification of Figure 6. Because of the similar result under the best condition at 500-3, the results for 4B system are selected as the separation criteria (Figure 7A), which correspond to the optimum separation condition. Obviously, Y_1 decreases with the increasing of partition coefficient K_1, which indicates that the separation can be achieved easily with the increasing of partition coefficients, and this result is in consistent with some golden rules given by Ito[1] such as, the suitable K values for HSCCC are $0.5 \leq K \leq 1.0$ considering the long separation time when K is bigger than 1.

In some conditions, the baseline separation is hard to achieve, so acceptable resolution ($Rs \geq 1$) is considered as well. As a result, Eq. 40 becomes

$$2(t_2 - t_1) \geq (w_2 + w_1) \tag{45}$$

And similarly,

$$Y_2 = 2 \times \sqrt{2\left(A \cdot \left(\frac{1}{\varepsilon K_2} + 1\right)^2 + B \cdot \left(1 + \frac{1}{K_2}\right)\right)} + 2 \times \sqrt{2\left(A \cdot \left(\frac{1}{\varepsilon K_2} + \frac{K_1}{K_2}\right)^2 + \frac{B \cdot K_1}{K_2^2}(K_1 + 1)\right)} + \frac{K_1}{K_2} \leq 1. \tag{46}$$

Thus, when $Y_2 \leq 1$, acceptable separations between two peaks can be achieved. According to the method described aforementioned for Y_1, the relationship between Y_2 and the partition coefficient ratio K_2/K_1 can be obtained as shown in Figure 7B. The baseline separation criterion Y_1 and acceptable separation criterion Y_2 can be readily read in Figure 7 when the partition coefficients K_1 and K_2 are available. For example, when the less retained substance K_1 has a partition coefficient 0.1, corresponding to $K_1 = 0.1$ curve, and if K_2/K_1 equals to 1.8, the Y_1 value on $K_1 = 0.1$ curve is 1.1 as shown in Figure 7A, which is higher than 1, so the baseline separation cannot be achieved. Then, the corresponding Y_2 value on Figure 7B is about 0.91, which is less than 1. Thus, we can know acceptable separation can be achieved. Figure 7 provides the straightforward information about whether the substances can be separated or not with known partition coefficients K_1 and K_2.

In a more quantitative way rather than reading Figure 7, critical values of separation criteria (Table 3) are calculated for the optimum separation condition (500-3) from Eqs. 41 and 46. From Table 3, when the partition coefficient of the less retained solute K_1 in one solvent system is 0.05, only if the partition coefficient ratio K_2/K_1 is more than 2.72, a baseline separation can be achieved under the optimum operating condition, and when the partition coefficient ratio K_2/K_1 is larger than 2.1, an acceptable separation is obtained; otherwise, the solvent system is not suitable for the separation of the two substances no matter what operating condition is. Table 3 only shows the separation criteria between 0 and 2, as for an efficient separation, the partition coefficient

Table 3. Separation Criteria in HSCCC

K_1 (Smaller Partition Coefficient)	K_2/K_1 for $Rs \geq 1.5$	K_2/K_1 for $Rs \geq 1$
0.05	2.72	2.11
0.1	1.98	1.64
0.2	1.61	1.39
0.3	1.48	1.31
0.5	1.38	1.24
0.6	1.36	1.23
0.7	1.34	1.22
0.8	1.32	1.21
0.9	1.30	1.20
1.0	1.29	1.19
2.0	1.25	1.16

Table 4. Comparison of Separation in HSCCC

Solvent System	Solutes	Partition coefficient (K)	K_2/K_1	Criteria Value: $Rs \geq 1.5$, Yes	Criteria Value: $Rs \geq 1$, Acceptable	Calculated Results: Yes/ Acceptable/ No	Experimental Results: Yes/ Acceptable/ No	Column Volume (ml)
n-Hexane–ethyl-acetate–*n*-butanol-methanol–water (0.5%TFA) (2:3:1:1.5, v/v)	Compound 2	0.52						325[33]
	Compound 3	0.54	0.54/0.52 = 1.04	1.38	1.24	No	No	
	Compound 4	0.65	0.65/0.54 = 1.20	1.37	1.24	No	No	
	Compound 5	1.31	1.31/0.65 = 2.02	1.35	1.225	Yes	Yes	
Chloroform–methanol–water (4:3:2, v/v)	Compound 4	0.49						
	Compound 2	0.81	0.81/0.49 = 1.65	1.38	1.24	Yes	Yes	
	Compound 3	1.08	1.08/0.81 = 1.33	1.32	1.21	Yes	Yes	
n-Hexane–ethyl acetate–methanol–water (11:9:10:10, v/v)	Aurantio-obtusin	0.78						350[34]
	1-Desmethylaurantio-obtusin	0.97	0.97/0.78 = 1.24	1.32	1.21	Acceptable	Acceptable	
	Chryso-obtusin	1.05	1.05/0.97 = 1.08	1.29	1.19	No	No	
	Obtusin	1.33	1.33/1.05 = 1.27	1.29	1.19	Yes	Yes	
	1-Desmethylchryso-obtusin	1.96	1.96/1.33 = 1.47	1.28	1.18	Yes	Yes	
Ethyl acetate–ethanol–water (4:1:5, v/v)	Chlorogenic acid	0.59						700[32]
	Caffeic acid	1.06	1.06/0.59 = 0.80	1.36	1.23	Yes	Yes	
	Luteolin	2.43	2.43/1.06 = 2.29	1.29	1.19	Yes	Yes	
Ethyl acetate–*n*-BuOH–water (2:3:5, v/v)	DIBOA-Glc	0.62						300[35]
	HBOA-Glc	0.67	0.67/0.62 = 1.08	1.36	1.23	No	No	
Ethyl acetate–*n*-BuOH–0.5% NH4OH (2:3:5, v/v)	DIBOA-Glc	0.03						
	HBOA-Glc	0.72	0.72/0.03 = 24	2.72	2.11	Yes	Yes	
n-Hexane–ethyl acetate–methanol–water (1:0.4:1:0.4, v/v)	Honokiol	0.78						36[28]
	Magnolol	1.46	1.46/0.78 = 1.87	1.32	1.21	Yes	Yes	
Light petroleum–ethyl acetate–methanol–water (9:1:8:2, v/v)	1	0.52						325[36]
	2	0.92	0.92/0.52 = 1.77	1.38	1.24	Yes	Yes	
HEMW (3:2:3:2, v/v)	I	0.20						325[37]
	II	0.70	0.70/0.20 = 3.5	1.61	1.39	Yes	Yes	
	III	0.87	0.87/0.70 = 1.24	1.34	1.22	Acceptable	Acceptable	
	IV	2.26	2.26/0.87 = 2.60	1.31	1.20	Yes	Yes	
	V	3.96	3.96/2.26 = 1.75	1.25	1.16	Yes	Yes	
n-Hexane–ethyl acetate–methanol–water (1:2:1:2, v/v_	I	0.11						290[38]
	II	0.45	0.45/0.11 = 4.09	2.0	1.65	Yes	Yes	
	III	0.83	0.83/0.45 = 1.84	1.45	1.26	Yes	Yes	
	IV	1.65	1.65/0.83 = 1.99	1.32	1.21	Yes	Yes	
	V	3.50	3.50/1.65 = 2.12	1.26	1.17	Yes	Yes	
Ethyl acetate–*n*-butanol–1% aqueous acetic acid (1:4:5, v/v)	1	1.02						325[39]
	2	1.80	1.80/1.02 = 1.76	1.29	1.19	Yes	Yes	
Ethyl acetate–*n*-butanol–1% aqueous acetic acid (5:0.5:5, v/v)	2	0.04						
	1	0.06	0.06/0.04 = 1.5	2.72	2.11	No	No	
	3	2.01	2.01/0.06 = 33.5	2.70	2.10	Yes	Yes	
	4	3.13	3.13/2.01 = 1.56	1.25	1.16	Yes	Yes	
n-Hexane–ethyl acetate–ethanol–water (1:0.6:1:0.6, v/v)	I	0.75						342[40]
	II	1.11	1.11/0.75 = 1.48	1.33	1.215	Yes	Yes	
	III	3.11	3.11/1.11 = 2.80	1.28	1.18	Yes	Yes	
	IV	6.10	6.10/3.11 = 1.96	1.25	1.16	Yes	Yes	
n-Hexane–ethyl acetate–ethanol–water (1:1:1:1, v/v)	I	0.45						
	II	0.58	0.58/0.45 = 1.288	1.40	1.29	No	No	
	III	1.25	1.25/0.58 = 2.16	1.36	1.23	Yes	Yes	

(*Continued*)

Table 4. (Continued)

Solvent System	Solutes	Partition coefficient (K)	K_2/K_1	Criteria Value: $Rs \geq 1.5$, Yes	Criteria Value: $Rs \geq 1$, Acceptable	Calculated Results: Yes/ Acceptable/ No	Experimental Results: Yes/ Acceptable/ No	Column Volume (ml)
	IV	2.66	2.66/1.25 = 2.13	1.28	1.18	Yes	Yes	
Ethyl acetate–*n*-butanol–water (2:1:3, v/v)	I	0.58						210[41]
	II	0.89	0.89/0.58 = 1.53	1.36	1.23	Yes	Yes	
	III	1.84	1.84/0.89 = 2.07	1.30	1.20	Yes	Yes	
Petroleum ether–ethyl acetate–ethanol–water (6:4:5:8, v/v)	Component 1	0.424						1000[42]
	Component 2	0.642	0.642/0.424 = 1.51	1.41	1.30	Yes	Yes	
	Component 3	0.817	0.817/0.642 = 1.27	1.35	1.225	Acceptable	Acceptable	
	Component 4	1.20	1.2/0.817 = 1.47	1.32	1.21	Yes	Yes	
n-Hexane–ethyl acetate–methanol–water (3:6:4:2, v/v)	Component 1	0.42						1000[43]
	Component 2	0.76	0.76/0.42 = 1.81	1.41	1.39	Yes	Yes	
	Component 3	1.39	1.39/0.76 = 1.83	1.33	1.22	Yes	Yes	

values of the targeted compounds should be $0.5 \leq K \leq 1.0$[11] in HSCCC. Moreover, it is widely believed that the partition coefficient ratio (separation factor K_2/K_1) should be greater than 1.5,[1,31,32] which is a rough value for predicting the separation, whereas from the results in Table 3, we can get the exact value for the targeted compounds with different partition coefficients. It is much more convenient to select the solvent system and optimize the separation by using the separation criteria in Table 3.

Comparing the model results to literature data

The separation results using the separation criteria (Table 3) were compared with the literature data[28,32–43] in Table 4. The first column shows the solvent system used for the separation of the solutes (in the second column "solutes"). The partition coefficient ratios K_2/K_1 were calculated based on the partition coefficient data in the third K column. For the first example in Table 4, it can be found that the partition coefficient ratio K_2/K_1 for the Compounds 2 and 3 is 0.54/0.52 = 1.04, that is, to divide the partition coefficient of the Compound 3 by that of the less retained Compound 2. According to the criteria value for $K_1 = 0.52$ shown in the fifth column, the separation criterion value is 1.38 for Rs $\geq$ 1.5 and 1.24 for Rs $\geq$ 1.0. K_2/K_1 of 1.04 is less than 1.38 or even 1.24, which indicates that even acceptable separation of the Compounds 2 and 3 cannot be achieved, so the calculated result "no" is shown in the "calculated results" column, which is the same as the experimental result shown in the "experimental results" column. Similarly, it can be found that the Compound 3 cannot be separated from the Compound 4 in *n*-hexane–ethyl acetate–*n*-butanol-methanol–water (0.5%TFA) (2:3:1:1.5, v/v) solvent system. Therefore, another solvent system chloroform–methanol–water (4:3:2, v/v) was used to separate these three Compounds 2, 3, and 4; the partition coefficient ratios for the Compounds 4 and 2, and the Compounds 2 and 3 are 1.65 and 1.33, respectively, which are higher than the criteria values (Rs $\geq$ 1.5) of 1.38 and 1.32, therefore, baseline separations can be achieved. Both the calculated and experimental results show "yes" for the successful separation. The results for the other 15 systems in Table 4 show that the agreement between the calculated and experimental data for different solvent systems and apparatuses including analytical (36 ml column volume), semipreparative (210–350 ml column volume), and preparative HSCCC (700 and 1000 ml column volume) is very good. These separation criteria provide some basic rules for choosing the suitable solvent systems, optimizing the operating condition. Comparing to the time- and solvent-consuming optimization process, these separation criteria allow us to optimize the HSCCC separation process in a quantitative and simple way, which is easy to use in practice by common user. Furthermore, Wood et al. reported that identical chromatograms can be achieved at both analytical and production scales.[44] Therefore, this separation criteria may apply to the production-scale HSCCC, but future work will be needed to verify this.

Conclusions

The TD model with parameters of the axial dispersion coefficient and the overall volumetric mass transfer coefficient was established for HSCCC based on the assumption that the peak broadening is caused by mass transfer and dispersion. One generalized correlation about volumetric mass transfer coefficients was derived based on the Schmidt (Sc) number, the rotational Reynolds number (Re_ω), and the partition coefficient (K). From the correlations of axial dispersion coefficients and volumetric mass transfer coefficients, the model proposed in this article predicted the elution concentration profile well for different HSCCC instruments including analytical, semipreparative, and preparative HSCCC. In addition, simple separation criteria based on the partition coefficients ratio (K_2/K_1) were proposed to predict the baseline separation ($Rs > 1.5$) and acceptable separation ($Rs > 1$) for two adjacent substances, and the agreement between the prediction and literature data for different solvent systems and different HSCCC apparatuses (analytical, semipreparative, and preparative) is very good. It is helpful for the selection and optimization of suitable separation conditions for HSCCC.

Acknowledgments

Financial support from the National Natural Science Foundation of People's Republic of China (project no: 20576113) and Zhejiang

Provincial Natural Science Foundation of China (project no: R4090358) is gratefully acknowledged.

Notation

a = specific interfacial area between the stationary and mobile phase, m^2/m^3
A = parameter defined in Eq. 42
A_c = cross-sectional area of the CCC column, m^2
A_{chrom} = chromatogram area
B = parameter defined in Eq. 43
b = a constant value defined in Eq. 10
C = solute elution concentration, g/ml
C_{cal} = calculated solute elution concentration, g/ml
C_{exp} = experimental solute elution concentration, g/ml
C_m = concentration of a solute in the mobile phase, g/ml
C_s = concentration of a solute in the stationary phase, g/ml
C_0 = concentration in feeds, g/ml
d = internal diameter of the column, m
D_{ax} = axial dispersion coefficients in the mobile phase, m^2/s, m^2/min
D_m = molecular diffusion coefficient, m^2/s, m^2/min
F = volumetric flow rate of the mobile phase, m^3/s or ml/min
k_0 = overall mass transfer coefficient, m/s
k_m = mass transfer coefficient in the mobile phase, m/s
k_s = mass transfer coefficient in the stationary phase, m/s
K = partition coefficient of solutes
L = total length of the column, m
M = sample mass, g
m_1 = parameter in Eq. 27
N = number of data points
r = the distance from the holder axis to the coil, m
R = revolution radius, m
Rs = peak resolution
Re = Reynolds number
Re_ω = rotational Reynolds number
s = surface renew factor
Sc = Schmidt number
Sh = Sherwood number
Sh' = modified Sherwood number
Sh'_m = modified Sherwood number in the mobile phase
S_f = retention of the stationary phase
Sum = sum of squared deviations
t = time or retention time, s, min
t_0 = sample loading time, s
t_1 = retention time of Solute 1, min or s
t_2 = retention time of Solute 2, min or s
u = mean velocity of the mobile phase, m/s
V_c = volume of the column, ml
V_{inj} = sample volume, ml
V_m = volume of the mobile phase, ml
V_s = volume of the stationary phase, ml
w_1 = peak width of Solute 1
w_2 = peak width of Solute 2
x = axial position in the column, m
x_1 = parameter in Eq. 16
x_2 = parameter in Eq. 16
x_3 = parameter in Eq. 16
Y_1 = parameter in Eq. 44
Y_2 = parameter in Eq. 46

Greek letters

μ = viscosity, Pa s
ω = rotation speed, rad/s
ρ = density, kg/m^3
β_r = ratio of the planetary radius to the rotor radius, r/R
ε = phase ratio of stationary phase volume to mobile phase volume
σ = [1/4] of peak width

Subscripts

m = mobile phase
s = stationary phase

Literature Cited

1. Ito Y. Golden rules and pitfalls in selecting optimum conditions for high-speed counter-current chromatography. *J Chromatogr A*. 2005;1065:145–168.
2. Kostanian AE. Modelling counter-current chromatography: a chemical engineering perspective. *J Chromatogr A*. 2002;973:39–46.
3. Kostanian AE, Berthod A, Ignatova SN, Maryutina TA, Spivakov BY, Sutherland IA. Countercurrent chromatographic separation: a hydrodynamic approach developed for extraction columns. *J Chromatogr A*. 2004;1040:63–72.
4. Sutherland IA, de Folter J, Wood P. Modelling CCC using an eluting countercurrent distribution model. *J Liq Chromatogr Relat Technol*. 2003;26:1449–1474.
5. vanBuel MJ, vanderWielen LAM, Luyben K. Effluent concentration profiles in centrifugal partition chromatography. *AIChE J*. 1997;43:693–702.
6. Marchal L, Legrand J, Foucault A. Mass transport and flow regimes in centrifugal partition chromatography. *AIChE J*. 2002;48:1692–1704.
7. Zhao CX, Xu YL, He CH. Axial dispersion coefficient in high-speed counter-current chromatography. *J Chromatogr A*. 2009;1216:4841–4846.
8. Ruthven DM. *Principles of Adsorption and Adsorption Processes*. New York: Wiley, 1984.
9. Suzuki M. *Adsorption Engineering*. Amsterdam: Elsevier, 1990.
10. Guiochon G, Shirazi SG, Katti AM. *Fundamentals of Preparative and Nonlinear Chromatography*. Boston, MA: Academic Press, 1994.
11. Sajonz P, GuanSajonz H, Zhong GM, Guiochon G. Application of the shock layer theory to the determination of the mass transfer rate coefficient and its concentration dependence for proteins on anion exchange columns. *Biotechnol Prog*. 1997;13:170–178.
12. Miyabe K, Guiochon G. Kinetic study of the concentration dependence of the mass transfer rate coefficient in anion-exchange chromatography of bovine serum albumin. *Biotechnol Prog*. 1999;15:740–752.
13. Miyabe K, Guiochon G. Kinetic study of the mass transfer of bovine serum albumin in anion-exchange chromatography. *J Chromatogr A*. 2000;866:147–171.
14. Kaczmarski K, Mazzotti M, Storti G, Morbidelli M. Modeling fixed-bed adsorption columns through orthogonal collocations on moving finite elements. *Comput Chem Eng*. 1997;21:641–660.
15. Berninger JA, Whitley RD, Zhang X, Wang NHL. A versatile model for simulation of reaction and nonequilibrium dynamics in multicomponent fixed-bed adsorption processes. *Comput Chem Eng*. 1991;15:749–768.
16. van Deemter JJ, Zuiderweg FJ, Klinkenberg A. Longitudinal diffusion and resistance to mass transfer as causes of nonideality in chromatography. *Chem Eng Sci*. 1956;5:271–289.
17. He CH, Zhao CX. Retention of the stationary phase for high-speed countercurrent chromatography. *AIChE J*. 2007;53:1460–1471.
18. Wood PL, Hawes D, Janaway L, Sutherland IA. Determination of J-type centrifuge extra-coil volume using stationary phase retentions at differing flow rates. *J Liq Chromatogr Relat Technol*. 2003;26:1417–1430.
19. Zhang CY, Werth CJ, Webb AG. A magnetic resonance imaging study of dense nonaqueous phase liquid dissolution from angular porous media. *Environ Sci Technol*. 2002;36:3310–3317.
20. Hong L, Gritti F, Guiochon G, Kaczmarski K. Rate constants of mass transfer kinetics in reversed phase liquid chromatography. *AIChE J*. 2005;51:3122–3133.
21. Perry RH, Green DW. *Perry's Chemical Engineers' Handbook*. Beijing: Science Press, 2001.
22. Danckwerts PV. Significance of liquid-film coefficients in gas absorption. *Ind Eng Chem*. 1951;43:1460–1467.
23. Wood PL, Hawes D, Janaway L, Sutherland IA. Stationary phase retention in CCC: modelling the J-type centrifuge as a constant pressure drop pump. *J Liq Chromatogr Relat Technol*. 2003;26:1373–1396.
24. Moustiri S, Hebrard G, Thakre SS, Roustan M. A unified correlation for predicting liquid axial dispersion coefficient in bubble columns. *Chem Eng Sci*. 2001;56:1041–1047.

25. Du QZ, Ke CQ, Ito Y. Separation of epigallocatechin gallate and gallocatechin gallate using multiple instruments connected in series. *J Liq Chromatogr Relat Technol*. 1998;21:203–208.
26. Chen JH, Wang FM, Lee FSC, Wang XR, Xie MY. Separation and identification of water-soluble salvianolic acids from *Salvia miltiorrhiza* Bunge by high-speed counter-current chromatography and ESI-MS analysis. *Talanta*. 2006;69:172–179.
27. Li HB, Chen F. Preparative isolation and purification of phillyrin from the medicinal plant *Forsythia suspensa* by high-speed counter-current chromatography. *J Chromatogr A*. 2005;1083:102–105.
28. Wang X, Liu JH, Zhang TY, Ito YC. Rapid and simple method for quality control of raw materials of herbs by HSCCC. *J Liq Chromatogr Relat Technol*. 2007;30:2585–2592.
29. Zhao CX, He CH. Preparative isolation and purification of atractylon and atractylenolide III from the Chinese medicinal plant *Atractylodes macrocephala* by high-speed counter-current chromatography. *J Sep Sci*. 2006;29:1630–1636.
30. Yan JZ, Tong SQ, Chu JJ, Sheng LQ, Chen G. Preparative isolation and purification of syringin and edgeworoside C from *Edgeworthia chrysantha* Lindl by high-speed counter-current chromatography. *J Chromatogr A*. 2004;1043:329–332.
31. Wang X, Li FW, Zhang HX, Geng YL, Yuan JP, Jiang T. Preparative isolation and purification of polymethoxylated flavones from Tangerine peel using high-speed counter-current chromatography. *J Chromatogr A*. 2005;1090:188–192.
32. Wang ZL, Wang JH, Sun YS, Li SB, Wang HZ. Purification of caffeic acid, chlorogenic acid and luteolin from Caulis Lonicerae by high-speed counter-current chromatography. *Sep Purif Technol*. 2008;63:721–724.
33. Xiao WH, Han LJ, Shi B. Isolation and purification of flavonoid glucosides from Radix Astragali by high-speed counter-current chromatography. *J Chromatogr B*. 2009;877:697–702.
34. Zhu LC, Yu SJ, Zeng XA, Fu X, Zhao MM. Preparative separation and purification of five anthraquinones from *Cassia tora* L. by high-speed counter-current chromatography. *Sep Purif Technol*. 2008;63:665–669.
35. Yin H, Zhang S, Luo XM, Liu YH. Preparative isolation and purification of two benzoxazinoid glucosides from *Acanthus ilicifolius* L. by high-speed counter-current chromatography. *J Chromatogr A*. 2008;1205:177–181.
36. Shi SY, Zhou HH, Huang KL, Li HB, Liu SQ, Zhao Y. Application of high-speed counter-current chromatography for the isolation of antiviral eremophilenolides from *Ligularia atroviolacea*. *Biomed Chromatogr*. 2008;22:985–991.
37. Peng AH, Li R, Hua J, Chen LJ, Zhao X, Luo HD, Ye HY, Yuan Y, Wei YQ. Flow rate gradient high-speed counter-current chromatography separation of five diterpenoids from *Triperygium wilfordii* and scale-up. *J Chromatogr A*. 2008;1200:129–135.
38. Yang CH, Tang QF, Liu JH, Zhang ZJ, Liu WY. Preparative isolation and purification of phenolic acids from Smilax china by high-speed counter-current chromatography. *Sep Purif Technol*. 2008;61:474–478.
39. Liu RM, Wu SA, Sun AL. Separation and purification of four chromones from radix saposhnikoviae by high-speed counter-current chromatography. *Phytochem Anal*. 2008;19:206–211.
40. Peng JY, Dong FQ, Ql Y, Han X, Xu YW, Xu LA, Xu QW, Liu KX, Zhu ZY. Preparative separation of four triterpene saponins from radix astragali by high-speed counter-current chromatography coupled with evaporative light scattering detection. *Phytochem Anal*. 2008;19:212–217.
41. Shi SY, Zhang YP, Zhao Y, Huang KL. Preparative isolation and purification of three flavonoid glycosides from *Taraxacum mongolicum* by high-speed counter-current chromatography. *J Sep Sci*. 2008;31:683–688.
42. OuYang XK, Jin MC, He CH. Preparative separation of four major alkaloids from medicinal plant of Tripterygium Wilfordii Hook F using high-speed counter-current chromatography. *Sep Purif Technol*. 2007;56:319–324.
43. Fan JP, He CH. Single-step preparative separation of barbinervic acid and its epimer (rotungenic acid), along with two other pentacyclic triterpene acids from the leaves of *Diospyros kaki* using HSCCC. *J Liq Chromatogr Relat Technol*. 2006;29:815–827.
44. Wood P, Ignatova S, Janaway L, Keay D, Hawes D, Garrard I, Sutherland IA. Counter-current chromatography separation scaled up from an analytical column to a production column. *J Chromatogr A*. 2007;1151:25–30.

Manuscript received Jun. 12, 2009, and revision received Mar. 8, 2010.